RECONSTRUCTING WAFER SURFACES WITH MODEL BASED SHAPE FROM SHADING

Alexander Nisenboim
Israel Institute of Technology, Applied Mathematics Dept., Haifa, Israel

Alfred Bruckstein
Israel Institute of Technology, Comuter Science Dept., Haifa, Israel

Keywords: Shape from shading, wafer, scanning electron microscope, mathematical model, wavelets, non-linear optimization.

Abstract: Model based Shape From Shading (SFS) is a promising paradigm introduced by J. Atick for solving such inverse problems when we happen to have some prior information on the depth profiles to be recovered. In the present work we adopt this approach to address the problem of recovering wafer profiles from images taken by a Scanning Electron Microscope (SEM). This problem arises naturally in the microelectronics inspection industry. A low dimensional model based on our prior knowledge of the types of depth profiles of wafer surfaces has been developed and based on it the SFS problem becomes an optimal parameter estimation. Wavelet techniques were then employed to calculate a good initial guess to be used in Levenberg-Marguardt (LM) minimization process that yields the desired profile parametrization. The proposed algorithm has been tested under both Lambertian and SEM imaging models.

1 INTRODUCTION

The problem of recovering a 3D object's shape from its shaded image, namely the Shape From Shading (SFS) problem, has intrigued the computer vision researchers for more then 30 years. The research in this area was mostly inspired by the fact that our brain has an outstanding ability to perceive the depth of the observed scene from 2D images on the retina. Shading is only one of the clues used by our brain to do the job. It is interesting that despite the lack of our understanding of this cognitive feature and major difficulties of our mathematical modeling attempts, nowadays there is a need for SFS-based applications in some branches of the computer industry. Manufacturing of integrated circuit wafers is an expensive and delicate process and a great deal of effort is invested in the control of quality and acceptability of such crucial device features as contact holes, tracks etc. Typically, the manufacturers are interested in measuring the geometrical parameters of the features and due to the "nano-sizes" of the structures studied, the non-destructive Low-Voltage SEM is used. Thus, the necessity of 3D-surface measurements from 2D SEM images naturally arises. The very nature of the SFS idea is to exploit the fact that the variations of surface's orientation cause the variations of the brightness at corresponding areas in the image. However, the brightness only carries information about the projection of surface normal on the light source direction (see eq. (1)) and hence the surface normal at each point cannot be uniquely discovered. Thus, mathematically speaking, the SFS problem appears to be ill-posed, however recent interesting reformulations challenge this viewpoint (Prados et al., 2004). One way to overcome these fundamental difficulties is to reformulate the SFS as a variational problem while introducing regularization terms into the minimized functional (Horn and Brooks., 1986), (Zheng and Chellappa, 1991). There are also alternative general approaches using facet model (T. Pong and Shapiro., 1989), level sets (R. Kimmel and Bruckstein., 1995) or hierarchical representations (A. Jones, 1994). However, being general, these approach could suffer from some drawbacks (A. Jones, 1994). In this work, following a paradigm introduced by J. Atick (Atick et al., 1996), we try to directly use a priori information about the geometry of the studied surfaces. Giving up gener-

Nisenboim A. and Bruckstein A. (2007).
RECONSTRUCTING WAFER SURFACES WITH MODEL BASED SHAPE FROM SHADING.
In *Proceedings of the Second International Conference on Computer Vision Theory and Applications - IU/MTSV*, pages 333-340

ality, we assume a model of the surface controlled by a finite set of parameters. The resulting parameter estimation SFS problem appears to be simpler than the original one. The initial estimates are obtained by means of analysis of the wavelet decomposition of the given image and subsequently a parameter fitting process is carried out. Finally, an iterative LM minimization procedure has been adopted in our work in order to insure stable numerical convergence. It should be mentioned here that this research was initiated and partially sponsored by Applied Materials,Inc., so the real data is banned from being published due to its high business sensitivity. Therefore the whole method is explained using a synthetic but illustrative example. This paper is organized as follows. In Section 2 we mathematically formulate the SFS problem and briefly overview the previous relevant work. Section 3 contains the description of the new method. Section 4 presents results and discussion.

2 THE SHAPE FROM SHADING PROBLEM

2.1 General Problem Setup

The monocular SFS problem is defined as follows. Suppose we are looking for a smooth height field $z = z(x,y)$ over region $D \subset \mathbb{R}^2$, and we are given its shaded image $I(x,y)$. The value of I at each point depends on reflectance properties of the surface, its gradient and imaging geometry parameters like light direction e.t.c. This dependence is called a reflectance function, and we denote it $R = R(p,q)$, where $p = z_x$ and $q = z_y$. The relationship

$$I(x,y) = R\left(p(x,y), q(x,y)\right) \tag{1}$$

is called the irradiance equation and we state the SFS problem as an attempt to recover the surface height field $z(x,y)$ from a single shaded image $I(x,y)$ given the reflectance function R, i.e. to determine $z(x,y)$ that satisfies (1). Some assumptions are to be made about imaging geometry. First, we assume that the size of the studied object is small, compared to the viewing distance, which enables us to presume orthographic projection to the image plane. We also assume that the camera direction coincides with the Z axis. In this case one can choose the coordinate system of both image and object planes to be identical and denoted by (X,Y). We denote η to be composite albedo which essentially captures the energy dissipation properties of the surface. We assume that η is constant along the surface. We also denote $\vec{L}$ to be the unit vector of the illumination direction. We assume that there is only one source of light located at infinity.

2.2 Imaging Models

By definition, if $R(p,q) = \eta < \vec{n}(x,y), \vec{L} >$ we say that a surface exhibits Lambertian diffuse reflection property. Here $<,>$ is a standard inner product and $\vec{n}(x,y) = (-p,-q,1)/\sqrt{p^2+q^2+1}$ is a unit normal vector to the surface. In case of SEM, the simplest image formation model is given by $R(p,q) = \eta / < \vec{n}(x,y), \vec{L} >$. This model holds well when specimen is coated by gold and in absence of charging artifacts (Reimer, 1993). It turns out that the problem of computing η and $\vec{L}$ can be solved separately (Zheng and Chellappa, 1991) and, therefore, we suppose them to be known. We should note here that the algorithm presented below in no way depends on any particular imaging model.

2.3 Previous Work

The problem of SFS was stated by B. Horn in 70's (Horn, 1975). His first solution involved characteristic strips expansion of the irradiance equation (1) and was not stable in practice due the noise sensitivity and error accumulation problems. During 80's, Horn and others (Horn and Brooks., 1986), (Zheng and Chellappa, 1991) reformulated the problem and solved it using the calculus of variations. Nice and comprehensive analysis of other SFS techniques can be found in (Zhang et al., 1999). Another important idea was suggested by J. Atick (Atick et al., 1996). In this work the authors dealt with the problem of recovering of the shape of human faces from their shaded images. In order to employ the a priori information about the class of objects studied, Atick gives up generality (of the variational approach) and solves the SFS problem for this particular class. The exact laser scans of 200 faces represented in a cylindrical coordinate system $\{r_i(\theta,l)\}_{i=1}^{200}$ where regarded as independent realizations of some stochastic process. Thus a "face-surface" can be represented as

$$r(\theta,l) = r_0(\theta,l) + \sum_{i=1}^{M} a_i u_i(\theta,l) \tag{2}$$

where $r_0(\theta,l)$ is a "mean-face", and $u_i(\theta,l)$ are the first M components of Karhunen-Loeve decomposition derived from the scanned surfaces, so-called "eigen-faces". So, denoting $\vec{\alpha} = (\alpha_1, \alpha_2, \ldots, \alpha_M)$ the SFS problem can be reformulated as

$$\min_{\vec{\alpha}} \sum_{l,\theta} \left(I\left(x(l,\theta), y(l,\theta)\right) - R(p,q;\vec{\alpha})\right)^2 \tag{3}$$

This basically means that we are looking for the best coefficients of the linear combination of the "eigenfaces" that explain our input image in terms of mean square error. Thus the SFS problem becomes one of optimal parameter estimation and it has been solved using gradient descent method.

3 MODEL BASED SFS FOR WAFERS

3.1 A Priori Knowledge

Unlike the work of J. Atick mentioned above, with surfaces of wafers no statistical information is available. Therefore we concentrate our efforts to employ a priori knowledge about wafer geometry in attempt to work out low-dimensional and meaningful representations of wafer surfaces. Wafer surface could be characterized as a plane with a set of mutually disjoint contact holes and tracks (Figure 1) which should subsequently be filled with conducting matter. These tracks might be either straight or bent. One can assume that the edges of holes and tracks are parallel to the X and/or Y axes of the image plane. This assumption does not always hold in practice, but its violation is rather rare and hence disregarded in our model. The shape of holes may vary with their size. Holes of relatively large size look like a rectangle with somewhat rounded corners and edges which are normally parallel to the axes. However, smaller holes assumed to have rather rounded shape like ellipses or circles. One cannot assume that slopes of holes and tracks are symmetrical. In the next section we define mathematical objects which fit well the geometry described above.

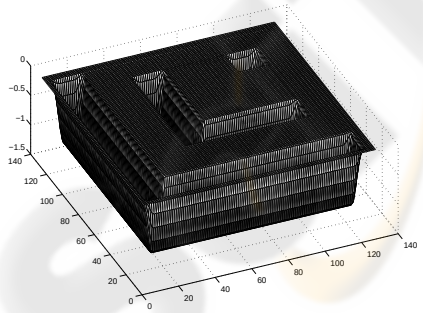

Figure 1: Wafer surface.

3.2 Mesa Function

We start with the following formal construction of a so-called mesa (table) function. Let us define

$$f(x;x_0,\varepsilon)=\begin{cases} c\exp\left(\dfrac{1}{1-\left(\frac{x-x_0}{\varepsilon}\right)^2}\right) & , \quad |x-x_0|<\varepsilon \\ 0 & , \quad \text{elsewhere} \end{cases} \tag{4}$$

The constant c in this definition is such that

$$\int_{x_0-\varepsilon}^{x_0+\varepsilon} f(x;x_0,\varepsilon)dx = 1 \tag{5}$$

Then a mesa function is then defined as

$$F(x;x_r,\varepsilon_r,x_l,\varepsilon_l)=\int_{-\infty}^{x}(f(t;x_l,\varepsilon_l)-f(t;x_r,\varepsilon_r))dt \tag{6}$$

The parameters of mesa function have simple geometrical interpretation:

1. $|x_r-x_l|$ is responsible for the size of the "pulse".
2. $\varepsilon_r,\varepsilon_l$ control the slopes of the function.

Now, let us define 2D mesa function of height h to be h times tensor product of two 1D mesa functions. For simplicity we denote

$$\vec{\alpha}_x=(x_r,\varepsilon_{xr},x_l,\varepsilon_{xl});\quad \vec{\alpha}_y=(y_r,\varepsilon_{yr},y_l,\varepsilon_{yl})$$

$$\vec{\alpha}=(x_r,\varepsilon_{xr},x_l,\varepsilon_{xl},y_r,\varepsilon_{yr},y_l,\varepsilon_{yl},h)=(\vec{\alpha}_x,\vec{\alpha}_y,h)$$

and then

$$T(x,y;\vec{\alpha})=h\cdot F(x;\vec{\alpha}_x)\cdot F(y;\vec{\alpha}_y)$$

See Figure 2.

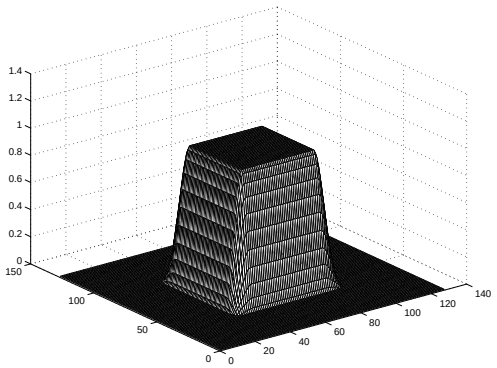

Figure 2: 2D mesa function.

3.3 Surface Representation

By means of 2D mesa functions we can build successful representations of surfaces of the type described in the previous section. Indeed, a straight track or hole feature can be represented as a negative 2D mesa function. A bent track, for example, can be constructed as difference of two 2D mesa functions when one of them is shifted from another. Therefore we can write

$$z(x,y) = \sum_{i=1}^{N} T_i(x,y), \tag{7}$$

when

$$T_i(x,y) = T(x,y;\vec{\alpha}_i)$$

which means that in terms of this model, SFS problem becomes one of optimal parameter estimation. In the following sections we shall develop a technique to separate between the features and find N initial sets of parameters (along with N itself) for each feature instead attempting to estimate them all together.

3.4 Strategy

It is well known that in order to succeed in the minimization process mentioned above a good initial estimate is needed. Let us briefly describe our main strategy. It is very common practice to take into account prior knowledge about image structure (like edge-geometry, or statistics of the noise e.t.c.) to simplify the very complex tasks of image processing and analysis. In our case, the surface model implies a certain geometrical structure of the image. First, all edges are straight and parallel to the axes. Second, the edges are expected to be organized in well-defined constellations. For example, in case of an image of a relatively large contact hole, its edges will tend to form a rectangular shape. See Figure 3. Therefore, by decomposing the image in Haar wavelets basis, and picking the largest amplitude coefficients one can get compact and effective representation of image singularities. Moreover, large Haar coefficients will carry the spatial information of image singularities at each level of the decomposition. Since image singularities form well-organized clusters, so do the large amplitude wavelet coefficients.Thus the wavelets representation properties could be exploited in order to localize every surface feature from its coefficients cluster and roughly calculate its parameter vector.This vector will subsequently serve as the starting point for the Least Square Error (LSE) optimization process and iteratively refined toward the final result.
Two points are worth mentioning. First, applying this strategy we will separate surface features and treat

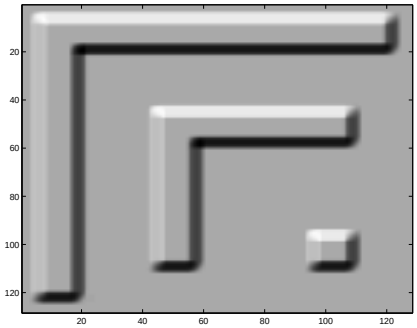

Figure 3: Lambertian image of the surface shown on Figure 1.

them independently which solves the problem of unknown number of terms in model (7). Second, the initial parameter estimates are geometrically meaningful which significantly reduces our chances to fall into some local minima during the LSE procedure. Let us elaborate on this strategy in the following sections.

3.5 Haar Wavelets for Tracking Singularities

The expansion of $I(x,y) \in L^2(\mathbb{R}^2)$ in the orthonormal basis of Haar functions $\left(\Psi^1_{j,n}, \Psi^2_{j,n}, \Psi^3_{j,n}\right)_{j\in\mathbb{Z}, n\in\mathbb{Z}^2}$

$$I(x,y) = \sum_{k=1}^{3} \sum_{j=-\infty}^{\infty} \sum_{n} w^k_{j,n} \Psi^k_{j,n} \tag{8}$$

where

$$w^k_{j,n} = \left\langle f, \Psi^k_{j,n} \right\rangle$$

will be referred as Discrete Haar Transform (DHT) and it has an interpretation in terms of image details aggregation at all resolution levels that range from 0 to $+\infty$, (Mallat, 1999). The inner products $w^1_{j,n}$ represent details in the horizontal direction, $w^2_{j,n}$ give the details in vertical direction and $w^3_{j,n}$ are the details in both directions (corners)(Fig. 4). It is suitable rectangular shape of Haar functions which makes them appealing to our model, since they should correlate well with mesa functions.Suppose that at each resolution scale s three binary images H_s, V_s and D_s, are produced (Fig. 5). The images are built from the large amplitude coefficients corresponding to horizontal, vertical and diagonal directions by means of binarization process. For any binary image B we denote $CC(B) = \{CC_i(B)\}$ to be the set of connected components of B. Then let us define a Feature Tracking Graph (FTG) G_s using the following definitions:

1. The set of vertices of G_s is equal to the set $CC(D_s)$.

2. The unordered pair (v_p, v_q) of vertices is said to be H-type edge if

$$\exists k:\ CC_p(D_s) \cap CC_k(H_s) \neq 0$$

and

$$CC_q(D_s) \cap CC_k(H_s) \neq 0$$

or V-type edge if

$$\exists k:\ CC_p(D_s) \cap CC_k(V_s) \neq 0$$

and

$$CC_q(D_s) \cap CC_k(V_s) \neq 0$$

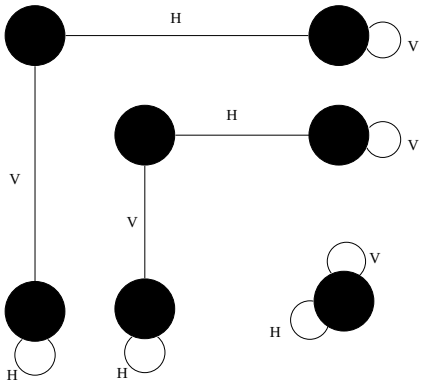

Figure 6: FTG built from the images illustrated on Fig 5.

Note that the operation $\cap$ should be redefined here because, $CC_p(D_s)$ and, for example, $CC_k(H_s)$ are embedded in different images. One can imagine that H_s, V_s and D_s are placed "one on top of the other", or in other words, they share the same coordinate system. In this sense the operation $\cap$ is well defined. Unconnected FTG G_s can be decomposed to the set of N connected subgraphs $G_s = \{CSG_i(G_s)\}_{i=1}^{N}$ by means of any standard method. Decomposition of FTG in connected subgraphs naturally reflects the geometrical structure of singularities at each level of resolution. For each $CSG_i(G_s)$ it is possible to locate the spatial position of the surface singularities which originated the coefficients that $CSG_i(G_s)$ is built from, and hence the number N of connected subgraphs is our estimate of number of terms in model (7). In order to trace the location of surface features we need a notion of the Spatial Orientation Trees (SOT) borrowed from the work of Shapiro (Shapiro., 1986). In this work so-called Zero Tree (ZT) have been used as a tool to optimize the transformation coefficients coding. Here we slightly modify ZT construction in order to adopt it to our goals. For each spatial orientation $k = 1,2,3$ we create quad-trees by relating recursively each coefficient at the scale s and position (p,q), say $w_s^k(p,q)$, to its four children at the next, finer, scale $s+1$: $w_{s+1}^k(2p,2q), w_{s+1}^k(2p+1,2q), w_{s+1}^k(2p,2q+1), w_{s+1}^k(2p+1,2q+1)$ Usually, the branching rule of the coefficients at the most coarse scale, say $s=0$, is different. Each coefficient $w_0^0(p,q)$ is associated with the three wavelet coefficients at the same scale and location: $w_0^1(p,q)$, $w_0^2(p,q)$, $w_0^3(p,q)$, and considered to be the roots of the trees.We artificially attach the image planes to each spatial orientation. The reason behind it is that we are going to use not the values of the pixels, but only their absolute coordinates. The "pseudo-coefficients" at this artificial level on the image plane will be considered as the leaves of the trees. The construction of SOT is illustrated in Figure 7. Note that if at some scale level s and position

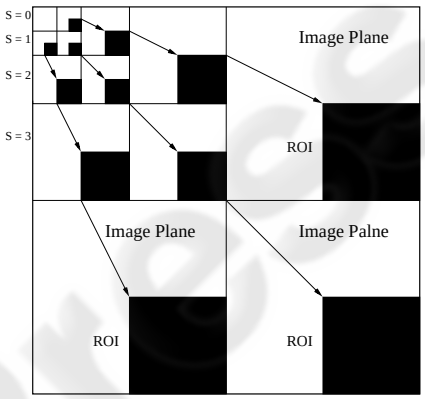

Figure 7: Spatial Orientation Tree.

(p,q) there is a wavelet coefficient $w_s^k(p,q)$ of high amplitude, then all image singularities which possibly contributed to the coefficient are likely to be included into the spatial area of the leaves of the SOT rooted at (s,p,q). Let us denote it as the region of influence of $w_s^k(s,p,q)$ by ROI(s,p,q), see Figure 7. Clearly, the wavelet coefficients $w_s^1(p,q)$, $w_s^2(p,q)$ and $w_s^3(p,q)$ have the same ROI. Now, the ROI of each connected subgraph can be defined as

$$\mathrm{ROI}\,(CSG_i(G_s)) = \bigcup_{(p,q)\in P_i(G_s)} \mathrm{ROI}(s,p,q) \qquad (9)$$

where $P_i(G_s)$ is the set of all points in H_s, V_s and D_s which constitute the connected subgraph $CSG_i(G_s)$. One can also see that by construction of the SOT the ROI's of two different points (s,p_1,q_1) and (s,p_2,q_2) are disjoint, and hence so are the ROI's of two different connected subgraphs. Thus, the decomposition of the graph G_s to the mutually disjoint connected subgraphs enables us to define a set of mutually disjoint domains on the image plane where the potential surface features are located. Then, it is possible to calculate the set of the initial guesses for the feature location in order to initialize the optimization process.We

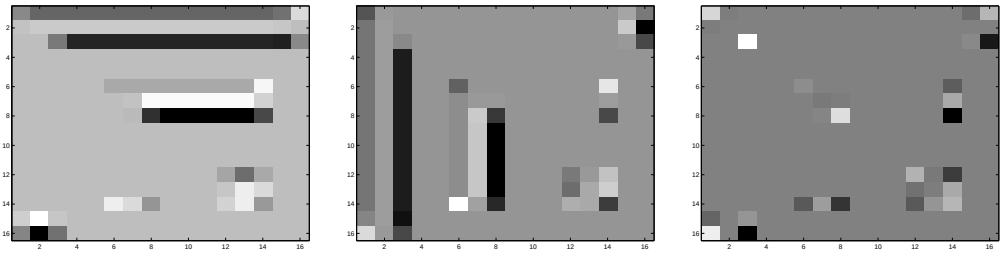

(H) (V) (D)

Figure 4: One scale of HDT of the image on Fig. 3.

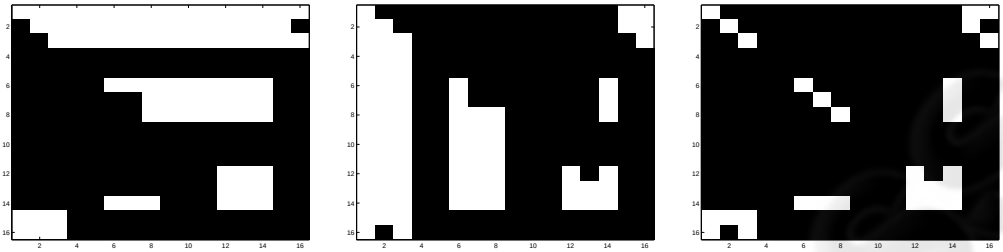

H_s V_s D_s

Figure 5: Binarization of the images displayed of Fig. 4.

use a rather simple strategy to establish the initial estimates for the surface parameters. Given the sets of mutually disjoint connected subgraphs and their ROIs we apply the following two-step heuristic decision:

S 1: Decide on the type of the feature (track/hole). For example, number of vertices and types of edges of $CSG_i(G_s)$ could be used.

S 2: Given the ROI, try to compute the parameters of a symmetrical feature of an appropriate type such that it would fully occupy the ROI. See Fig. 8.

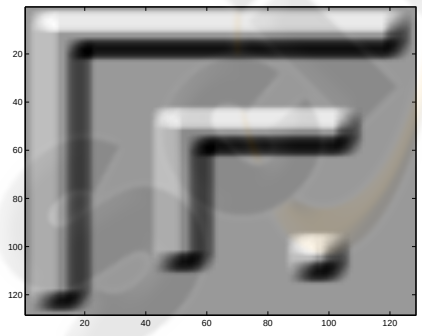

Figure 8: Image of the initial guess.

The only parameter which does not play any role in this heuristic decision is the parameter h of the 2D mesa-function. We suggest to overcome this problem by choosing the initial value of the parameter according to the available data from the CAD of the wafer. Let us also amplify the following advantage of the proposed method. Since the ROIs are mutually disjoint the optimization computations could be carried out in parallel and his may provide considerable speed-up in such a heavy computational task as SFS.

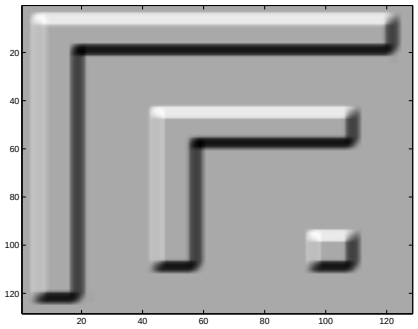

Figure 9: Lambertian image of the surface reconstructed by our method from noise free image.

3.5.1 The Sfs Algorithm

We present the summary of our new SFS algorithm.

Input: 1. $I(x,y)$ - input image.
2. S - the coarsest scale level of DHT.
3. LET - the local error tolerance.

Output: 1. Number of features found.
2. A vector of parameters of each feature.
3. A vector of local errors induced by the calculated vector of the parameters.

S 1: 1.1 Compute HDT of $I(x,y)$ up to scale level S.
1.2 Set the current scale level $s = 1$.

S 2: 2.1 Produce three binary images H, V and D at the current scale s.
2.2 If the images H, B and D are zero - STOP.

S 3: 3.1 Build the connected components of H, V and D.
3.2 Build the graph G_s.
3.3 Compute $\{CSG_i(G_s)\}_{i=1}^{N}$

S 4: For each connected subgraph do
4.1 Decide on its type.
4.2 Calculate ROI $(CSG_i(G_s))$.
4.3 Calculate the initial estimate vector $\vec{\alpha}_0$.
4.4 Launch LM procedure on the ROI starting with $\vec{\alpha}_0$, to determine

$$\min_{\vec{\alpha}} \sum_{(x,y)\in \mathrm{ROI}} (I(x,y) - R(x,y;\vec{\alpha}))^2$$

4.5 Save the resulting vector of parameters and the error introduced by it.
4.6 If the error is less then the LET
4.6.1 For each pixel $(p,q) \in P_i(G_s)$ set all the wavelet coefficients in the SOT rooted at (s,p,q) to zero.
4.6.2 Output the resulting vector and the error.

S 5: 5.1 Set $s = s+1$.
5.2 If $s > S$ — STOP, otherwise GOTO Step 2.

It is worth mentioning LM scheme is one of the most widely used non-linear data fitting methods, and it is often described in the literature, see e.g. (Gill et al., 1982).

4 RESULTS AND DISCUSSION

There are several important characteristics of the algorithm which we shall subsequently point out.As we build the DHT pyramid from the fine to the coarse scale levels, the connected components of high amplitude coefficients tend to mix together, meaning, that the geometrical information carried by them is much more precise on the fine levels of the pyramid. Actually, if the image is absolutely free of noise it is sufficient to choose $S = 1$ to recover the surface. However, in the presence of additive white noise the geometrical information is likely to "survive" at higher levels. Note that if a feature has been recovered from some coarse level s of the pyramid and some connected subgraph $CSG_i(G_s)$, then there is no point in taking into account the wavelet coefficients from finer levels belonging to the SOTs rooted at $(p,q) \in P_i(G_s)$. That is why the auxiliary step 4.6.1 has been introduced. In order to demonstrate the efficiency and accuracy of the proposed algorithm the SFS method based on variational approach has been implemented to provide data for the performance comparisons. The images of resulting surfaces are displayed on Figures 9 and 10, when the image on Fig. 3 has been used as an input for both methods. We also consider the case when the input image is contaminated by additive Gaussian noise. The advantage of using DHT from noise robustness standpoint becomes obvious when one observes the reconstruction using the binarized DHT of the noisy input image displayed on Figure 11. Here we apply Gaussian noise with $mean = 0$ and $variance = 0.01$. One can see that in the presence of additive white noise, no comprehensible information will be contained at the finest level of the pyramid, see Figure 11 H_1, V_1 and D_1. On the other hand the information is still available from the level corresponding to $s = 3$, i.e. Figure 11 H_3, V_3 and D_3. Subsequently, the initial estimation and the following minimization will not be badly affected by the noise. The image of the surface reconstructed from the noisy data is displayed on Figure 12. Finally, error comparison between model based and variational methods is given on Figure 13.

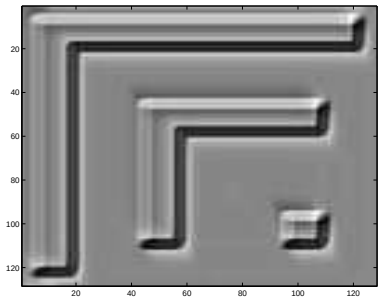

Figure 10: Lambertian image of the surface reconstructed using variational approach from noise free image.

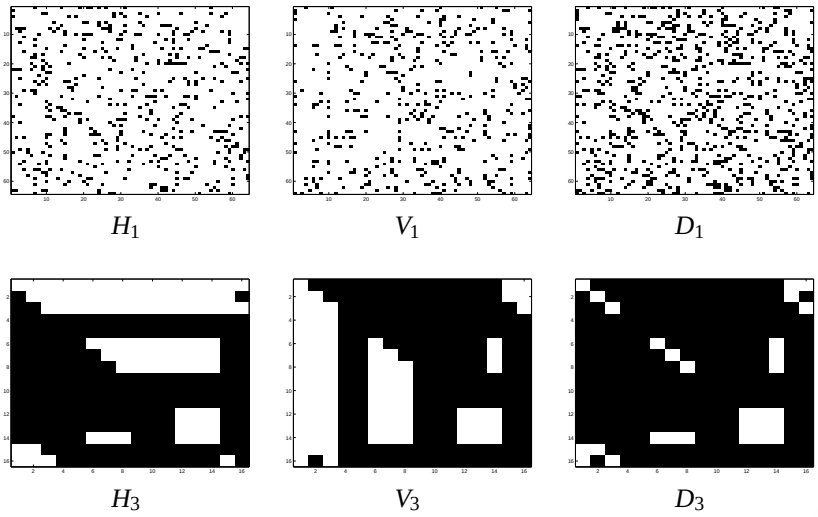

Figure 11: *Binarization of the DHT of the noisy image.*

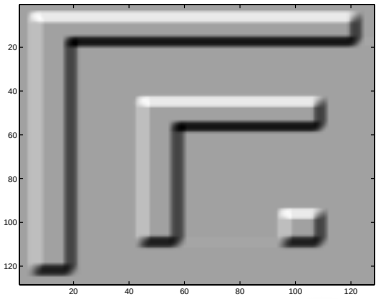

Figure 12: Image of the surface reconstructed from noisy data by our method.

Method, Data type	Errors, STD	
	Brightness	Depth
Our method, noise free	0.45	0.06
Our method, noisy	0.54	0.48
Variational method, noise free	2.73	2.12

Figure 13: *Error comparison.*

ACKNOWLEDGEMENTS

The generous support of Applied Materials Inc. is thankfully acknowledged.

REFERENCES

A. Jones, G. T. (1994). Robust shape from shading. In *Image and Vision Computing, vol 12, no. 7. pp 411-421.*

Atick, J., Griffin, P., and Redlich, A. (1996). Statistical approach to shape from shading, reconstruction of three-dimensional face surface from single two-dimensional images. In *Neural Computation 8, pp 1321-1340.*

Gill, P., Murray, W., and Wright, M. (1982). *Practical Optimization.* Academic Press, London.

Horn, B. (1975). Obtaining shape from shading information. In *Psychology of Computer Vision. pp 115-155.*

Horn, B. and Brooks., M. (1986). The variational approach to shape from shading. In *Computer Vision, Graphics and Image Processing, vol 33, no. 1. pp 174-208.*

Mallat, S. (1999). *A Wavelet Tour of Signal Processing.* Academic Press, London, 2nd edition.

Prados, E., Faugeras, O., and Camilli, F. (2004). Shape from shading: a well-posed problem ?. In *INRIA, Tech. Report. RR-5297.*

R. Kimmel, K. Siddiqi, B. K. and Bruckstein., A. M. (1995). Shape from shading: Level set propagatioin and viscosity solutions. In *International Journal of Computer Vision, vol 16, no. 1. pp 107-133.*

Reimer, L. (1993). *Image Formation in Low-Voltage Scanning Electron Microscopy.* SPIE Press, Bellingham, USA.

Shapiro., J. (1986). Embedding image coding using zerotrees of wavelet coefficients. In *IEEE Trans. on Signal Processing, vol 41, no. 12. pp 3445-3462.*

T. Pong, R. H. and Shapiro., L. (1989). Shape from shading using the facet model. In *Pattern Recognition, vol 22, no. 6. pp 683-695.*

Zhang, R., Tsai, P., Cryer, J., and Shah., M. (1999). Shape from shading: A survey. In *IEEE Trans. PAMI Vol.21, No. 8 pp 690-706.*

Zheng, Q. and Chellappa, R. (1991). Estimation of illuminant direction, albedo and shape from shading. In *IEEE Trans. on PAMI, vol. 13, no. 7, pp 680-7021.*